Eur. Phys. J. C 21, 545–555 (2001)
Digital Object Identifier (DOI) 10.1007/s100520100728

THE EUROPEAN PHYSICAL JOURNAL C

The strange border of the QCD phases

S. Kabana[a]

Laboratory for High Energy Physics, University of Bern, 3012 Bern, Switzerland

Received: 17 April 2001 /
Published online: 24 August 2001 –

Abstract. We address the flavour composition along the border between the hadronic and the quark–gluon plasma phases of QCD. The ratio of strange to up and down antiquarks (λ_s) produced in particle and nuclear collisions is found to increase in collisions with an initially reached energy density (ϵ_i) up to $\epsilon_{\rm crit} \sim 1\,{\rm GeV/fm}^3$. Above this value it decreases approximately linearly and reaches its asymptotic value at zero baryon chemical potential ($\mu_{\rm B}$). We demonstrate that λ_s in nuclear collisions approaches its asymptotic value at $\epsilon_i \sim 8$–$9\,{\rm GeV/fm}^3$, corresponding to $s^{1/2} \sim 3$–$8\,{\rm TeV}$ per nucleon + nucleon pair, which will be reached at the LHC. After correcting for the difference in the chemical potentials of various colliding systems, λ_s universally saturates across the QCD phase boundary, following the temperature. Recent experimental puzzles as the increase in the K^+/π^+ ratio in Pb + Pb collisions at 40 GeV per nucleon, its different behaviour at midrapidity, the decrease of the double ratio of $K/\pi(A+A/p+p)$ in nucleus–nucleus over $p+p$ collisions with increasing $s^{1/2}$, and the increase of λ_s in $p+A$ over $p+p$ collisions at the same $s^{1/2}$, are naturally explained. We study the approach of thermodynamic observables at $\mu_{\rm B}=0$ to the transition point and extract an estimate of the critical temperature.

1 Introduction

One outstanding prediction of the theory of strong interaction (see, e.g., [1–4]), which applies to the evolution of the early universe, is the phase transition from confined hadrons to a deconfined phase of their constituents, the quarks and gluons; the so-called quark–gluon plasma (QGP). An experimental program which started in the eighties and continues in many accelerators like CERN SPS, BNL RHIC and others, has been dedicated to the experimental verification of this transition [5–9]. The main process is nuclear reactions at high energy to achieve a thermalized state with temperature exceeding the critical temperature for the QCD phase transition. One of the predicted signatures of this change of phase is an enhancement of strange particles [10]. The main idea was

(a) the lower threshold for the production of $s\overline{s}$ quarks in the QGP through e.g. $gg \to s\overline{s}$ as compared to the higher threshold for production of strange hadrons in a hadronic reaction, like for example $pp \to p\Lambda K^+$, and
(b) the similarity of the mass of the strange quark with the critical temperature $T \sim 200\,{\rm MeV}$, which allows for the equilibration of strange quarks in the QGP.

Argument (a) holds for all quark flavours, leading to the conclusion that all hadron multiplicities are expected to be increased when produced out of a hadronizing QGP, as compared to hadron production out of a collision which does not pass through the QCD phase transition. The enhancement can be related in a simple way to phase space [11] and is flavour dependent.

However, the argument (b) is true only for the quarks which have mass less than or of the order of the critical temperature of approximately 200 MeV [4].

Therefore next to the up and down quarks, strange quarks are expected to play a crucial role in identifying the QCD phase transition. In particular, hadrons with $u, \overline{u}, d, \overline{d}, s$ and $\overline{s}$ quarks are expected to reflect the critical behaviour of a locally equilibrated phase made up of $u, \overline{u}, d, \overline{d}, s, \overline{s}$ quarks and gluons.

Heavier flavours like charm and beauty can be affected by the QCD transition in several ways as discussed in the literature [8,12,13]. They give important insights e.g. by the experimental measurement of the dissociation temperature of $c\overline{c}$ or $b\overline{b}$ states which can be at or above the critical one [8,12,14].

Therefore, since the dissociation of quarkonia may be due to overcritical energy densities, it appears that the critical parameters of the transition can be extracted only through other observables which are sensitive to the transition at the critical energy density and approximately frozen with fast hadronization, for example fluctuations of several parameters and multiplicities of hadrons which include up, down and strange quarks.

In this paper we concentrate on the behaviour of the strange flavour across the QCD phase boundary. The main point is to interpret the global features of the data (of $A+A$, $p\overline{p}$, e^+e^- collisions at $s^{1/2} = 2$–$1800\,{\rm GeV}$) within a strictly thermodynamic approximation, and not to repro-

[a] e-mail: sonja.kabana@cern.ch

duce the data in detail using models outside the validity of thermodynamics.

Clearly, no perfect global equilibration is reached in these systems which moreover are a mix of several thermodynamic reservoirs e.g. along the rapidity axis. It appears however that the hadrons in the final state of the colliding systems studied, do not rule out a thermodynamic description. This is especially the case when a centrality selection has been imposed.

Preliminary results of part of this work have been shown in [15].

In Sect. 2 we extract thermodynamic parameters $(T, \mu_{\rm B}, \mu_s)$ for fixed target Au + Au collisions at 2 and 4 GeV per nucleon and for fixed target Pb + Pb collisions at 40 GeV. In Sect. 3 we estimate the initial energy density reached in the collisions. In Sect. 4 we examine the strangeness suppression factor at non-zero chemical potentials as a function of the initial energy density, and find its asymptotic value using nuclear collisions. In Sect. 5 we extract the temperature at zero chemical potentials and draw the "strange border of the QCD phases". We discuss how the critical parameters for the transition are extracted and elaborate on the explanation of several recent experimental puzzles.

2 Thermodynamic description of nuclear collisions at 2, 4 and 40A GeV

We compare the ratios of experimentally measured hadron yields in nuclear collisions with the prediction of a grand canonical ensemble of non-interacting free hadron resonances. We consider the pseudoscalar and vector u, d, s meson nonets as well as the spin 1/2 baryon octet and spin 3/2 decuplet and their antiparticles as well as the $f_0(400$–$1200)$ or σ, interpreted as a scalar glueball [16]. We impose exact conservation of strangeness, and we correct for the change of final observed hadron yields due to decays of higher lying resonances (the so-called "feeding"). Further details of this model can be found in [4]. We extract then the thermodynamic parameters: temperature, baryochemical potential ($\mu_{\rm B}$) and strangeness chemical potential ($\mu_{\rm S}$) from the model prediction which describes the data best. We discuss in the following the production of strangeness relative to non-strange particles extracting the quantity: $\lambda_s = 2\overline{s}/(\overline{u} + \overline{d})$ which is a measure of the strangeness suppression factor defined and used in the literature as $\lambda_s = 2(s + \overline{s})/(u + \overline{u} + d + \overline{d})$ [17].

A similar analysis extracting thermal parameters from data can be found in the literature, e.g. [18–20,17,21–24]. For a recent review see [25].

A main new idea, introduced in [11,4] and used in this paper, is the extrapolation of all thermodynamic states to equivalent states at zero chemical potentials, e.g. along isentropic paths.

Throughout this paper, all parameters discussed concern the state of hadrons at their chemical freeze-out; that is at the time after which the hadron yields do not change anymore through inelastic collisions. The only exception is the initial energy density which refers to the early state of the system.

Table 1. Au + Au at $s^{1/2} = 2.3$ GeV. Predicted versus experimental particle ratios for the best fit of our model

Ratio	Model	Data
K/π	0.0110	0.00929 ± 0.00257
π/p	0.268	0.266 ± 0.0770
Λ/K^0_s	2.770	3.222 ± 2.274

2.1 Thermodynamic description of Au + Au collisions at 2A GeV

We use 3 ratios measured in fixed target Au+Au collisions at 2 GeV per nucleon beam energy as shown in Table 1 from [26,27] and impose strangeness conservation. The predicted and the experimental ratios are shown in Table 1. The K/π and the π/p ratios are measured at midrapidity, while the Λ/K^0_s ratio is measured nearby [26]. To account for the different phase space we add a 10% systematic error to the Λ/K^0_s ratio.

The resulting χ^2/DOF is (1.41/1) (CL 23%). After defining the (T, μ_b, μ_s) values describing the particle ratios produced in central Au + Au collisions at $s^{1/2} = 2.3$ GeV at the chemical freeze-out we extrapolate to the T at zero fugacities (Table 2) along an isentropic path.

2.2 Thermodynamic description of Au + Au collisions at 4A GeV

We use 4 ratios measured in fixed target Au + Au collisions at 4 GeV per nucleon beam energy as shown in Table 3 from [26,27] and impose strangeness conservation. The predicted and the experimental ratios are shown in Table 3.

The K/π, π/p and K^+/K^- ratios are measured at midrapidity, while the Λ/K^0_s ratio is measured nearby [26]. To account for the different phase space we add a 10% systematic error to the Λ/K^0_s ratio.

The resulting χ^2/DOF is (1.62/2) (CL $\sim$ 40%). After defining the (T, μ_b, μ_s) values describing the particle ratios produced in central Au + Au collisions at $s^{1/2} = 3.3$ GeV at the chemical freeze-out we extrapolate to the T at zero fugacities (Table 4) along an isentropic path.

2.3 Thermodynamic description of Pb + Pb collisions at 40A GeV

We use 5 ratios measured in Pb + Pb collisions at 40 GeV per nucleon beam energy as shown in Table 5 from [28,29] and impose strangeness conservation. The predicted and the experimental ratios are shown in Table 5.

The ratios $\overline{\Lambda}/\Lambda$, $\overline{\Xi}/\Xi$ are measured at midrapidity, while the other ratios are given in full phase space acceptance. The $(B - \overline{B})$ is taken equal to the total number of participant nucleons.

Table 2. Au + Au at $s^{1/2} = 2.3\,\mathrm{GeV}$. Thermodynamic parameters for the best fit and temperatures and λ_s extrapolated to zero fugacities

μ_b GeV	μ_s GeV	T GeV	λ_s	ρ_s $1/\mathrm{fm}^3$	$T(\mathrm{eq}, \rho_s)$ GeV	$\lambda_s(\mathrm{eq}, \rho_s)$
0.714	0.0918	0.0510 ± 0.006	0.0321 ± 0.0327	0.0435	0.072 $+0.032 - 0.013$	0.0388 $+0.116 - 0.0249$

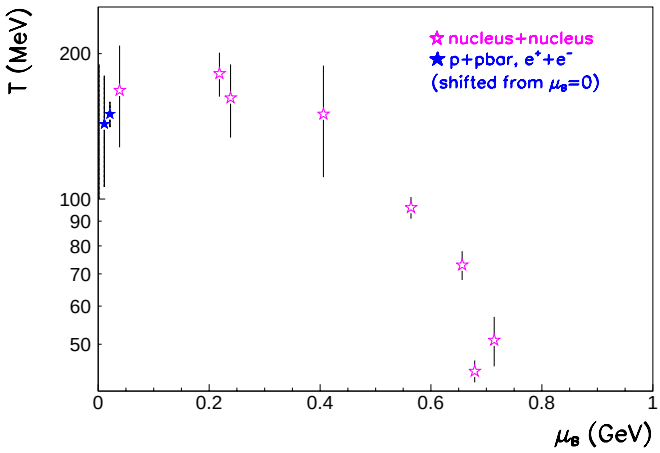

Fig. 1. The temperature as a function of the baryochemical potential for several nucleus + nucleus, hadron + hadron and lepton + lepton collisions. We demand for the fits a confidence level > 10%

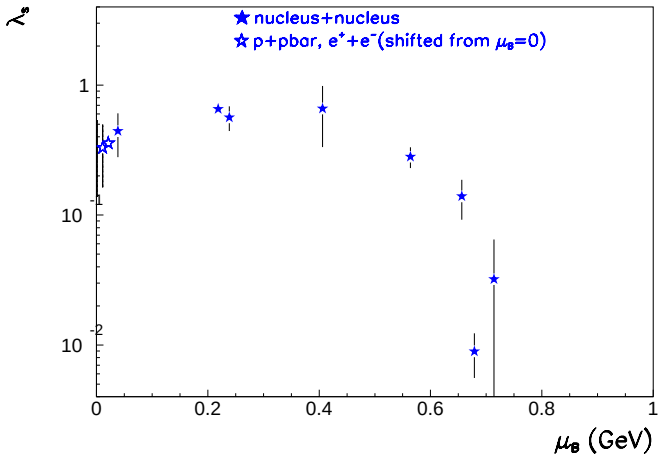

Fig. 2. The λ_s factor as a function of the baryochemical potential for several nucleus + nucleus, hadron + hadron and lepton + lepton collisions. We demand for the fits a confidence level > 10%

Table 3. Au + Au at $s^{1/2} = 3.3\,\mathrm{GeV}$. Predicted versus experimental particle ratios for the best fit of our model

Ratio	Model	Data
K/π	0.0396	0.0422 ± 0.0111
K^+/K^-	12.437	12.316 ± 0.699
Λ/K_s^0	2.342	2.750 ± 0.342
π/p	0.473	0.435 ± 0.114

To account for the different phase space and the use of the assumption $(B - \overline{B}) = N_{\mathrm{participant}}$ we add a 10% systematic error to the $\pi/(B - \overline{B})$, $\overline{\Lambda}/\Lambda$ and $\overline{\Xi}/\Xi$ ratios.

The resulting χ^2/DOF is (6.68/3) (CL $\sim$ 10%). After defining the (T, μ_b, μ_s) values describing the particle ratios produced in central Au + Au collisions at $s^{1/2} = 8.76\,\mathrm{GeV}$ at the chemical freeze-out we extrapolate to the T at zero fugacities (Table 6) along an isentropic path.

The correlation between the extracted thermodynamic parameters temperature (T), strangeness suppression factor (λ_s) and the chemical potentials of all systems together with results from [4], is shown in Figs. 1, 2, 3, 4, and 5.

3 Initial energy density estimation

We estimate the initial energy density for the collision systems studied in Sect. 2 by taking the nuclear energy

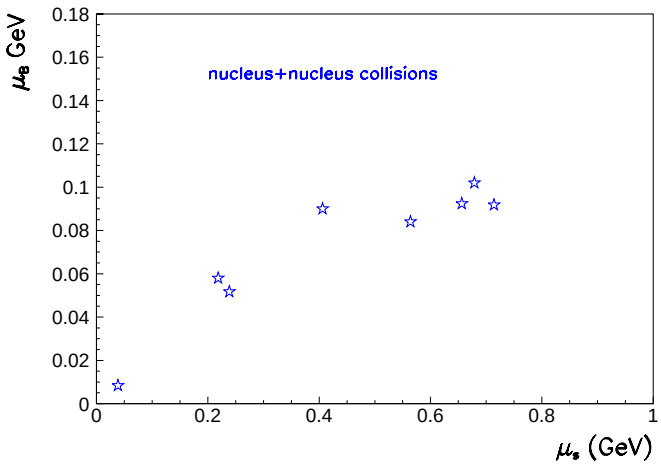

Fig. 3. The baryochemical potential as a function of the strangeness chemical potential for several nucleus + nucleus collisions. We demand for the fits a confidence level > 10%

density of two overlapping nuclei $2\epsilon_A$ times the γ factor of the colliding particles in the center of mass minus one:

$$\epsilon_\gamma = 2\epsilon_A(\gamma - 1), \tag{1}$$

with $\gamma = (s^{1/2}/2)/m_{\mathrm{nucleon}}$, and $\epsilon_A = 0.138\,\mathrm{GeV/fm}^3$ is the normal nuclear matter density. The value in (1) multiplied by the stopping power gives an estimate of the initial energy density available for heating. This formula is better suited for low energy data, for example AGS, where the

Table 4. Au + Au at $s^{1/2} = 3.3\,\mathrm{GeV}$. Thermodynamic parameters for the best fit and temperatures and λ_s extrapolated to zero fugacities

μ_b GeV	μ_s GeV	T GeV	λ_s	ρ_s $1/\mathrm{fm}^3$	$T(\mathrm{eq}, \rho_s)$ GeV	$\lambda_s(\mathrm{eq}, \rho_s)$
0.657	0.0923	0.073 ± 0.005	0.139 $+0.047 - 0.040$	0.163	0.097 $+0.016 - 0.009$	0.125 $+0.0710 - 0.0359$

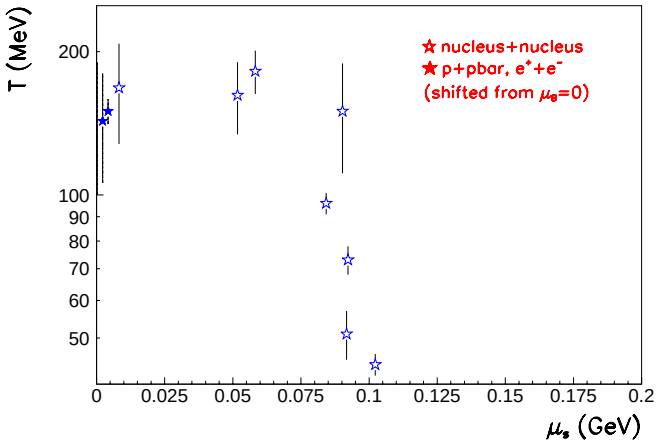

Fig. 4. The temperature as a function of the strangeness chemical potential for several nucleus+nucleus, hadron+hadron and lepton + lepton collisions. We demand for the fits a confidence level $> 10\%$

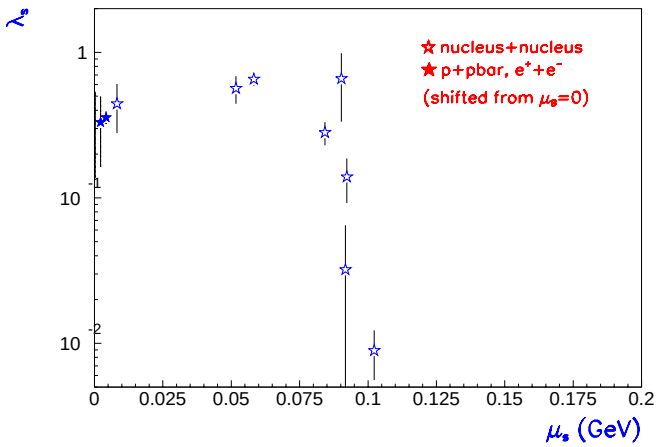

Fig. 5. The λ_s factor as a function of the strangeness chemical potential for several nucleus + nucleus, hadron + hadron and lepton + lepton collisions. We demand for the fits a confidence level $> 10\%$

applicability of the Bjorken formula [30] for the energy density calculation is questionable. For a discussion of the systematic error of $\sim$ 30–50% on the initial energy density calculation for nucleus–nucleus and particle collisions respectively, see [4,31].

The resulting initial energy densities are $\epsilon_{\mathrm{in}}(\mathrm{Au} + \mathrm{Au}; s^{1/2} = 2.3\,\mathrm{GeV}) = 0.12\,\mathrm{GeV/fm}^3$, $\epsilon_{\mathrm{in}}(\mathrm{Au} + \mathrm{Au}; s^{1/2} = 3.3\,\mathrm{GeV}) = 0.21\,\mathrm{GeV/fm}^3$, $\epsilon_{\mathrm{in}}(\mathrm{Pb}+\mathrm{Pb}; s^{1/2} = 8.8\,\mathrm{GeV}) = 1.01\,\mathrm{GeV/fm}^3$.

Table 5. Pb + Pb at $s^{1/2} = 8.76\,\mathrm{GeV}$. Predicted versus experimental particle ratios for the best fit of our model

Ratio	Model	Data
K/π	0.128	0.125 ± 0.0072
K^+/K^-	3.0355	3.163 ± 0.232
$\pi/(B - \overline{B})$	1.122	0.852 ± 0.125
$\overline{\Lambda}/\Lambda$	0.0216	0.0230 ± 0.00251
$\overline{\Xi}/\Xi$	5.146E − 2	8.00E − 2 ± 2.625E − 2

4 The energy density dependence of λ_s at finite μ

Two general comments are important for the understanding of the behaviour of strangeness in particle and nuclear collisions and our later discussion. Since collisions of protons and collisions of nuclei at the same energy per nucleon do reach different initial energy densities, it is proper to compare hadronic observables as a function of the initial energy density instead of $s^{1/2}$.

It is also a fact that in all investigated colliding systems with an initial non-zero net baryon number, the baryon and strangeness chemical potentials are non-zero and different. Next to the initial baryon number, also the energy of the collisions and hence the stopping influences the baryochemical potential of the final hadrons produced. Therefore the final state of the same nuclei, when colliding at different energies, will be described by different baryochemical potentials.

This leads to the conclusions that

(a) the behaviour of strangeness as a QGP signature can be discussed while comparing systems with the same baryon chemical potential, and
(b) the initial energy density is a better "critical" parameter than $s^{1/2}$, against which different colliding systems can be compared. We take these as starting points and study their consequences in the following discussion.

When comparing the strange to non-strange particle ratio in nucleus–nucleus collisions with $p + p$ collisions at the same energy an enhancement is seen, which increases with decreasing energy [32]. This observation is quantified in Fig. 6, taken from [29], which shows the ratio of $(\Lambda + \overline{\Lambda} + K)/\pi$ as a function of the variable F which is a function of the $s^{1/2}$ of the collision. The line shows a model prediction from [33] assuming that the phase transition occurs in the vicinity of the maximum. (For recent literature on the interpretation of data on strangeness see e.g. [34].)

In Fig. 7 the strangeness suppression factor λ_s is shown as a function of the initial energy density. The open stars

Table 6. Pb + Pb at $s^{1/2} = 8.76\,\text{GeV}$. Thermodynamic parameters for the best fit and temperatures and λ_s extrapolated to zero fugacities

μ_b GeV	μ_s GeV	T GeV	λ_s	ρ_s $1/\text{fm}^3$	$T(\text{eq}, \rho_s)$ GeV	$\lambda_s(\text{eq}, \rho_s)$
0.405	0.090	0.150 $+0.019 - 0.039$	0.660 $+0.138 - 0.326$	2.466	0.164 $+0.024 - 0.049$	0.407 $+0.068 - 0.199$

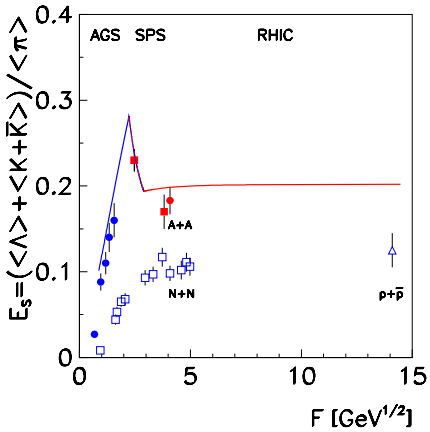

Fig. 6. $(\langle\Lambda\rangle + \langle K + \overline{K}\rangle)/\pi$ ratio as a function of $F = f(s^{1/2})$ in $A+A$ and $p+p$ collisions [29], compared with a model from [33]

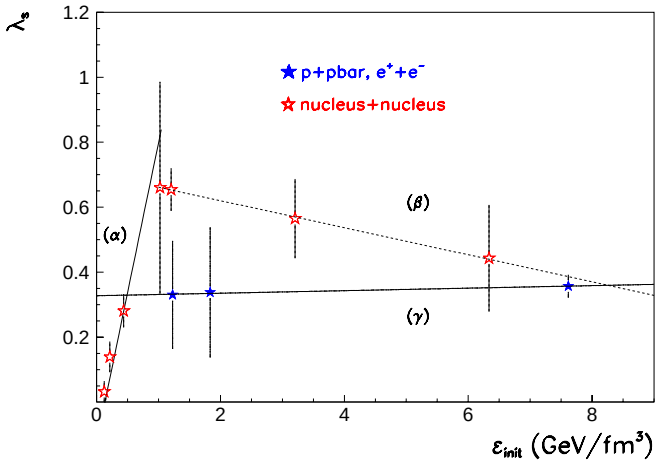

Fig. 7. The λ_s factor as a function of the initial energy density for several nucleus + nucleus, hadron + hadron and lepton + lepton collisions. We demand for the fits a confidence level $> 10\%$. The lines α and β show λ_s at non-zero μ_B, while the line γ shows λ_s at zero μ_B

show nucleus–nucleus collision results from the present analysis and the ones from [4], while the closed stars show results from $p\overline{p}$ and e^+e^- collisions from [4]. The lines shown are linear fits to the data points to illustrate the tendency of the data.

The λ_s points of all investigated nuclear collisions, define the λ_s behaviour at non-zero and varying chemical potentials (the two lines (α) and (β) of the upper half of the triangle shown). The horizontal line (γ) going through the $p\overline{p}$ and e^+e^- data defines the λ_s value at the zero chemical potentials in the ϵ_i region shown.

The λ_s factor grows reaching a maximum around $\epsilon_i \sim 1\,\text{GeV/fm}^3$ and then decreases continuously and almost linearly towards an asymptotic value which is defined by the curve with zero chemical potentials of the $p\overline{p}$ and e^+e^- data. Therefore it follows that no saturation of the λ_s value is reached at an energy density between $1\,\text{GeV/fm}^3$ and $8\,\text{GeV/fm}^3$ in nucleus–nucleus collisions, as the one indicated in Fig. 6.

We will argue that the phenomenon of enhancement of the λ_s value in nucleus collisions as compared to the λ_s values in elementary particle collisions, quantified in Fig. 7 by the area of the triangle, is mainly due to the difference in the baryochemical potential.

With increasing energy, the central rapidity region in nuclear collisions becomes increasingly net baryon free approaching a state of a nucleus + antinucleus collision.

This tendency is shown in Fig. 7 by the decrease of the line (α) with increasing ϵ_i. The statistical significance of the present data does not allow for a thorough investigation of the exact shape of the decrease. In particular, in order to find deviations from a linear behaviour, more data are needed.

The non-zero potential λ_s line (α) crosses the zero potential λ_s horizontal line (γ) at an initial energy density of $\sim$ 8–9 GeV/fm^3 (depending on the way we extrapolate, e.g. using a linear, exponential or a polynomial distribution). The linear fit crosses at $8.25\,\text{GeV/fm}^3$.

This indicates that the limiting value of λ_s (and an almost net baryon free midrapidity region) will be achieved at nuclear collisions reaching an initial energy density of $\sim$ 8–9 GeV/fm^3 [1]. Assuming that ϵ_i scales as the logarithm of $s^{1/2}$, we find that the $s^{1/2}$ needed to achieve the limiting value of λ_s using nucleus–nucleus collisions is approximately 3–8 TeV. This energy density could therefore be achieved by the Large Hadron Collider at CERN.

5 The energy density dependence of λ_s at zero μ

In the following we discuss the ϵ_i dependence of the λ_s factor after extrapolating all thermodynamic states with

[1] The net baryon free midrapidity region in a particle + particle collision and its equivalence with particle+antiparticle collision can probably be achieved only in the limit of infinite energy. We address here the question at which energy this asymptotic value is significantly approached within the errors

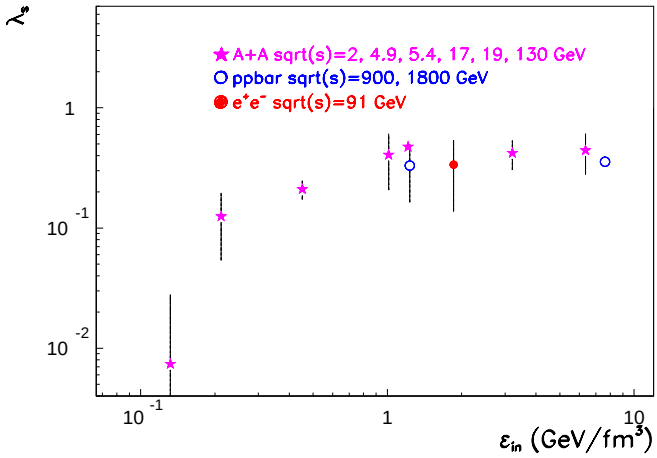

Fig. 8. The λ_s factor (in logarithmic scale) extrapolated to zero fugacities along an isentropic path, as a function of the initial energy density for several nucleus + nucleus, hadron + hadron and lepton + lepton collisions. We demand for the fits a confidence level $> 10\%$

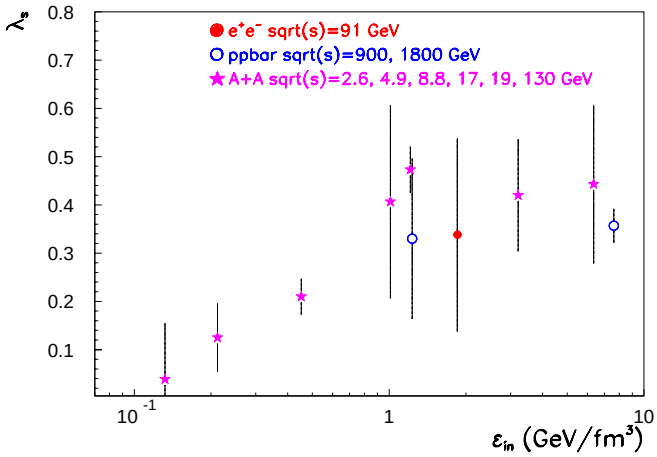

Fig. 9. The λ_s factor (in linear scale) extrapolated to zero fugacities along an isentropic path, as a function of the initial energy density for several nucleus + nucleus, hadron + hadron and lepton + lepton collisions. We demand for the fits a confidence level $> 10\%$

non-zero baryochemical potential to zero along an isentropic path. The result is shown in Fig. 8 in logarithmic representation and in Fig. 9 in linear representation. All λ_s values show a universal behaviour increasing from below until $\epsilon_i \sim 1\,\mathrm{GeV/fm^3}$ and then saturating.

Several comments can be made:

(1) The figure clearly demonstrates that the peak of λ_s and of E_s at $40A\,\mathrm{GeV}$ Pb + Pb collisions and their drop towards higher energies, seen in Figs. 6 and 7, is due to the non-zero baryochemical potential in the collisions. The λ_s factor is the same for Pb + Pb collisions at 40 and at $158A\,\mathrm{GeV}$ in Fig. 8 (4th and 8th points from the left).

Therefore, the so-called "strangeness suppression" phenomenon [29,35], that is, the decrease of the strange to non-strange particle ratios (e.g. K/π) from 40 GeV Pb + Pb towards 158 GeV Pb + Pb collisions is explained by the different baryochemical potentials of these systems.

This interpretation is supported by the difference seen in the $s^{1/2}$ dependence of the K^+/π^+ and the K^-/π^- ratio as a function of $s^{1/2}$ [29]. In particular, it is seen that the peak at $40A\,\mathrm{GeV}$ Pb + Pb colisions appears only in the K^+/π^+ ratio (K^+ is "forced" by the high μ_B to be abundantly produced in association with Λ).

(2) The increase of the double ratio $K/\pi(A + A/p + p)$ with decreasing $s^{1/2}$ discussed e.g. in the review talk [36] is a natural consequence arising from the above ideas[2].

From this comparison the apparent strangeness enhancement is increasing towards lower energies. However, the comparison leading to this conclusion is not taking into account the varying characteristic parameters.

(3) The K/π ratio is investigated in [35] and shows the above mentioned strangeness suppression with $s^{1/2}$, when constructed using yields of particles in the full phase space acceptance, while it remains constant at midrapidity.

This can be explained by the fact that the baryochemical potential reaches its lowest value at the midrapidity of nucleus–nucleus collisions and the highest one in the forward and backward rapidity regions (multiple reservoirs); see e.g. [37,38]. Therefore, when considering K/π at midrapidity the bias from non-zero μ_B is minimized as compared to full acceptance yields.

(4) The enhancement seen in strange to non-strange particle yields in central $p + A$ collisions when compared to $p + p$ at the same energy [39], is explained in the same way, since central $p + A$ collisions reach a higher μ and a higher initial energy density as $p + p$ collisions at the same $s^{1/2}$.

(5) The strangeness enhancement as defined in the literature (double ratio of λ_s in $A + A$ over $p + p$ collisions at the same $s^{1/2}$) and as illustrated in Fig. 6 finds the same explanation.

Normalizing to the same μ_B value (here chosen to be zero for simplicity) and comparing at the same initial energy density, the above mentioned "strangeness enhancement" disappears.

The λ_s factor for particle collisions is within the error compatible with nucleus–nucleus collisions as seen in Figs. 8 and 9.

(6) Enfin: what can we learn from strangeness production about the QCD phase transition?

First, Fig. 8 exhibits a very distinct feature of λ_s as a function of ϵ_i: λ_s is increasing with initial energy density increasing from 0.14 to $1\,\mathrm{GeV/fm^3}$. After this ϵ_i value, λ_s saturates at a limiting value of $\lambda_\mathrm{lim} = 0.365 \pm 0.033 \pm 0.07$ [4].

Second, this behaviour is followed universally by all collisions studied.

[2] The increase is of course large when the threshold for strangeness production in $p + p$ reactions is approached, while subthreshold strangeness production can still occur in nuclear collisions, but this limiting case is not the main point of the present discussion

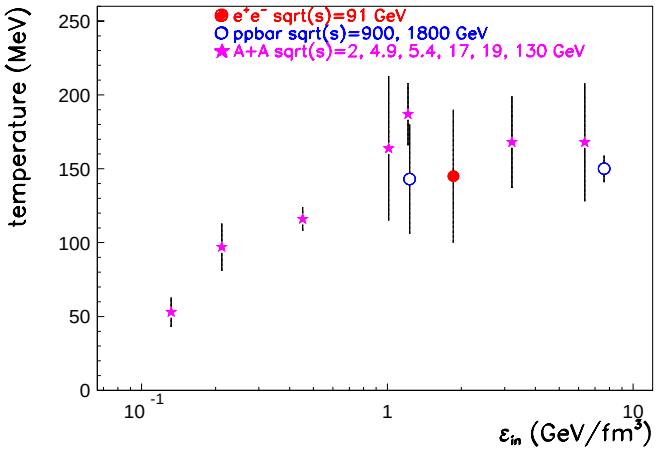

Fig. 10. The temperature extrapolated to zero fugacities along an isentropic path, as a function of the initial energy density for several nucleus + nucleus, hadron + hadron and lepton + lepton collisions. We demand for the fits a confidence level $> 10\%$

Third, λ_s is following closely the ϵ_i dependence of the temperature at the chemical freeze-out of hadrons (as shown in Fig. 10).

Assuming that local equilibrium conditions are reached in all collisions studied, and therefore that temperature is defined, we interpret the dramatic change of the temperature and of λ_s at chemical freeze-out near $\epsilon_i \sim 1\,\mathrm{GeV/fm^3}$, as critical behaviour: the onset of saturation occurs when the critical energy density for the QCD phase transition is reached[3].

The T as well as λ_s would continue to rise with ϵ_i if no phase transition occurs.

A bias in this interpretation is the implicit assumption that T does not cool down without noticing the transition due to some peculiar expansion dynamics and its $s^{1/2}$ dependence. However, in this case the cooling mechanism should generate the universal behaviour seen in Figs. 8 and 10 by coincidence.

Furthermore, since pressure and expansion characteristics have been measured to be different in different $A+A$ collisions (e.g. there are strong flow phenomena pointing to high initial pressure in $A+A$ collisions which are more pronounced at RHIC than in SPS, and not seen in $p+p$ collisions) it seems difficult to explain the universally flat temperature curve exhibited by all $p+p$ and $A+A$ data, by a non-universal expansion dynamics.

A phenomenon analogous to the one seen in Fig. 10 is the following: We fill a box with water and look for the water–vapour phase transition without tools to detect vapour. Each time the transition to vapour (= QGP) occurs we wait until the vapour condensates back to water (= hadron gas), in order to measure its temperature.

We make a plot of the water temperature as a function of the applied heat, and it looks like Fig. 10, namely it rises and saturates at the value of $\leq 100°\mathrm{C}$.

[3] A rise and subsequent saturation of the T has been discussed e.g. in [41]

Adding salt to water and repeating the experiment would result in different critical values, increasing with salinity.

The baryochemical potential is like salt for hadronic systems. To achieve measuring one single curve one has to use the same salinity, as we do in Figs. 10 and 8. As a result, the border of the QCD phase transition can be drawn and the critical energy density can be extracted self-consistently from the data, independent of any model predicting where the boundary must be.

The dependence of the temperature on the baryon and strangeness chemical potentials is shown in Figs. 1 and 4.

If all these points would lie exactly on the critical border, their extrapolation to equivalent states at zero potentials would lead to one single critical temperature.

If all points would not lie on the critical border but well below, their extrapolation to the equivalent states with μ_B zero would give scattered temperatures below the critical one, without showing signs of saturation.

One could argue against this that the saturation is caused by the freeze-out conditions and the critical temperature is never reached in the initial state (for example if there is no T_crit nearby).

In this case however, the freeze-out conditions should change with the collision energy, because the cross sections of particle interactions and the mean free path changes too with $s^{1/2}$. Again saturation is then coincidental.

A second argument against such coincidence is the following: If the freeze-out conditions do imply a universal temperature at chemical freeze-out then there should be no variation in the chemical freeze-out temperature at zero chemical potentials. That is, the plot of Fig. 10 should be completely flat for all thermal systems.

A third argument is the similarity of the critical parameters that we extract in the above described picture and in [4] with the expected critical parameters from QCD ($T_\mathrm{crit} \sim 200\,\mathrm{MeV}$, $\epsilon_\mathrm{crit} \sim 1\,\mathrm{GeV/fm^3}$ [4] and from other calculations too, e.g. from lattice simulations [1]). Even if the estimation of the initial energy density [30] has a large inherent error, e.g. in the assumption of a formation time of $1\,\mathrm{fm}/c$, still the error hardly amounts to a factor 7 (the difference between ϵ_i of Tevatron and the $\epsilon_i = 1\,\mathrm{GeV/fm^3}$). Also our limiting temperature determination is more reliable than the initial energy density estimate and yet T_lim and ϵ_crit agree reasonably with each other and with the QCD predictions. Finally, we conclude that Bjorken's estimate [30] turns out to be correct.

(7) It is important to note that while studying the λ_s or the temperature dependence on the initial energy density using their values at non-zero chemical potential (Fig. 7) one cannot extract the critical energy density nor the limiting temperature from this study, as they are shifted.

In particular, the values one can extract in this case simply reflect the fact that we deal with a critical border which is a 2-dimensional surface. However, more data are needed in order to observe this shift.

(8) All temperatures achieved with hadrons are below the critical temperature for sure; however, they can approach the border. We can measure only the approach to the crit-

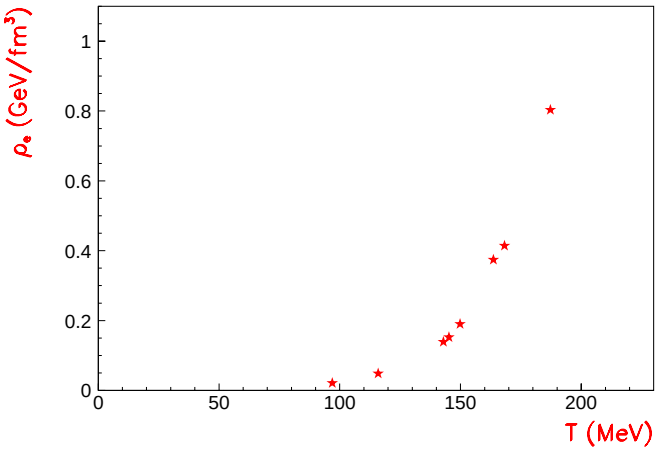

Fig. 11. The energy density ρ_e as a function of the temperature extrapolated to zero fugacities along an isentropic path for many nucleus + nucleus, hadron + hadron and lepton + lepton collisions. We demand for the thermal model fits a confidence level > 10%

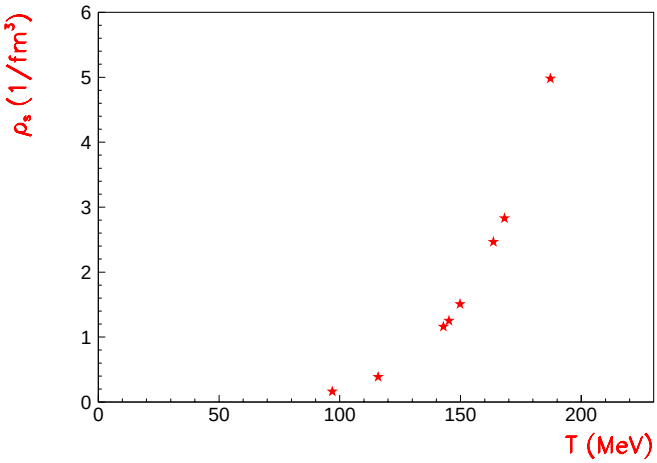

Fig. 12. The entropy density ρ_s as a function of the temperature extrapolated to zero fugacities along an isentropic path for many nucleus + nucleus, hadron + hadron and lepton + lepton collisions. We demand for the thermal model fits a confidence level > 10%

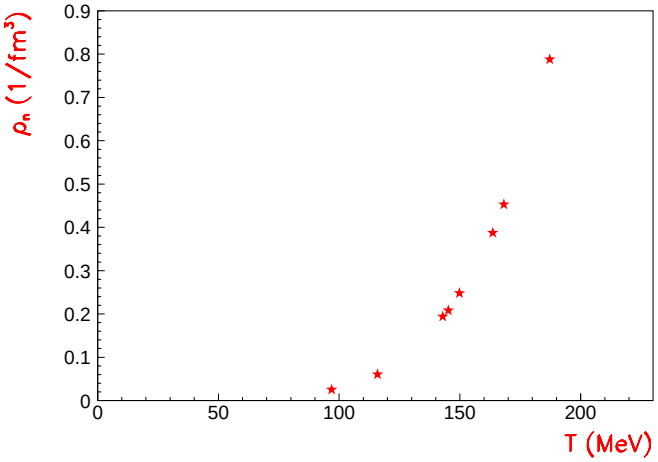

Fig. 13. The density ρ_n as a function of the temperature extrapolated to zero fugacities along an isentropic path for many nucleus + nucleus, hadron + hadron and lepton + lepton collisions. We demand for the thermal model fits a confidence level > 10%

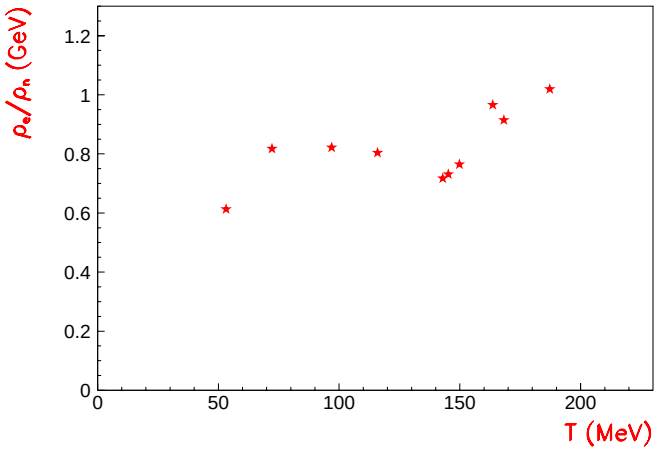

Fig. 14. The ratio of the energy density to the density as a function of the temperature extrapolated to zero fugacities along an isentropic path for many nucleus + nucleus, hadron + hadron and lepton + lepton collisions. We demand for the thermal model fits a confidence level > 10%

ical surface from the hadronic side, study the way the critical values are approached and extract the critical parameters from critical behaviour.

We assume that the QCD phase transition sets in at $\epsilon_i \sim 1\,\mathrm{GeV/fm^3}$ as suggested by Fig. 10. Therefore we display the parameters describing the measured colliding systems as functions of temperature at $\mu_\mathrm{B} = 0$, and study the way the systems approach the transition in Figs. 11, 12, 13, 14, 15, 16, 17, 18 and 19.

In Figs. 14 and 16 it is seen that the energy density over the particle density and the entropy density over the energy density show an onset of a critical behaviour at $T \sim 150\,\mathrm{MeV}$, while the entropy density over the particle density shown in Fig. 15 saturates above $T \sim 150\,\mathrm{MeV}$.

In Fig. 19 we try to fit the function $f = \beta[\ln(1./(1 - T/T_\mathrm{crit}))]^\alpha$ (logarithmic critical behaviour) to the data which go through the QGP phase transition according to Figs. 10 and 8 (that is, the points with $T \geq 145$), and extract the critical temperature $T_\mathrm{crit}^\mathrm{fit}$ and the critical exponent α^fit from the fit. We find a value for the critical temperature of $T_\mathrm{crit}^\mathrm{fit} = 218 \pm 70\,\mathrm{MeV}$, and an exponent $\alpha^\mathrm{fit} = 0.54 \pm 0.47$ with $\chi^2/\mathrm{DOF} = 0.059/3$. This behaviour cannot be studied with the precision of a study of the neighbourhood of the Curie point in ferromagnets [40].

This value for $T_\mathrm{crit}^\mathrm{fit}$ is in agreement with the QCD expectations for the critical temperature of $T_\mathrm{crit}^\mathrm{th} = 194 \pm 18\,\mathrm{MeV}$ [4].

6 Conclusions

The starting point of this paper is the extraction of thermodynamic parameters describing the final state of Au +

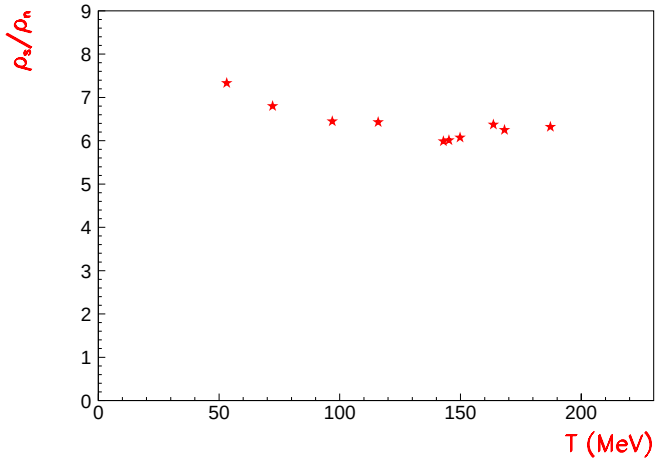

Fig. 15. The ratio of the entropy density to the density as a function of the temperature extrapolated to zero fugacities along an isentropic path for many nucleus + nucleus, hadron + hadron and lepton + lepton collisions. We demand for the thermal model fits a confidence level > 10%

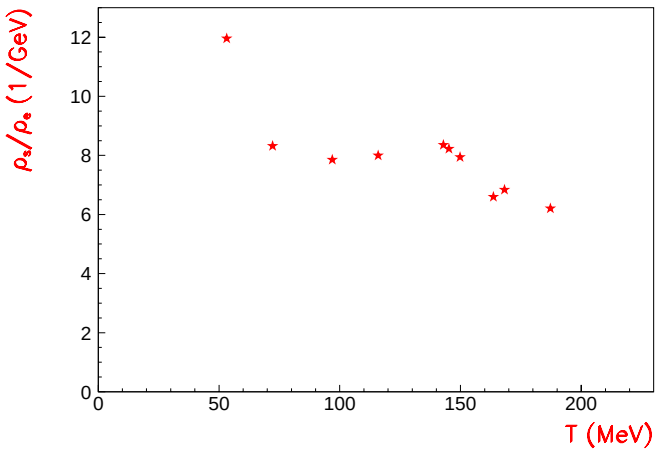

Fig. 16. The ratio of the entropy density to the energy density as a function of the temperature extrapolated to zero fugacities along an isentropic path for many nucleus + nucleus, hadron + hadron and lepton + lepton collisions. We demand for the thermal model fits a confidence level > 10%

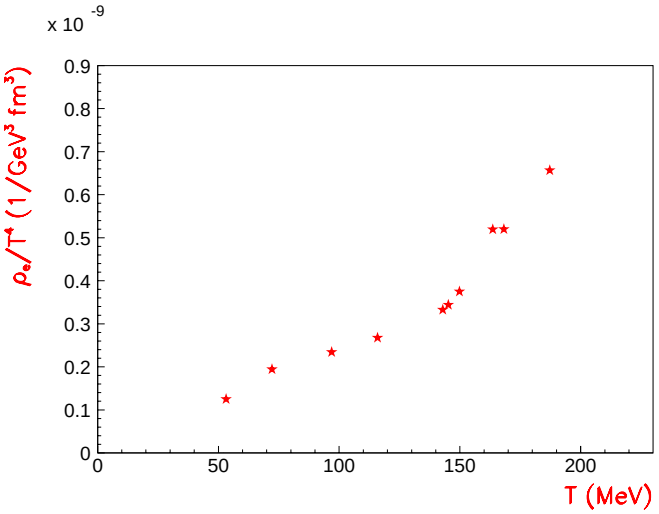

Fig. 17. The ratio of the energy density to the temperature to the 4th power as a function of the temperature. The temperature is extrapolated to zero fugacities along an isentropic path for many nucleus+nucleus, hadron+hadron and lepton+lepton collisions. We demand for the thermal model fits a confidence level > 10%

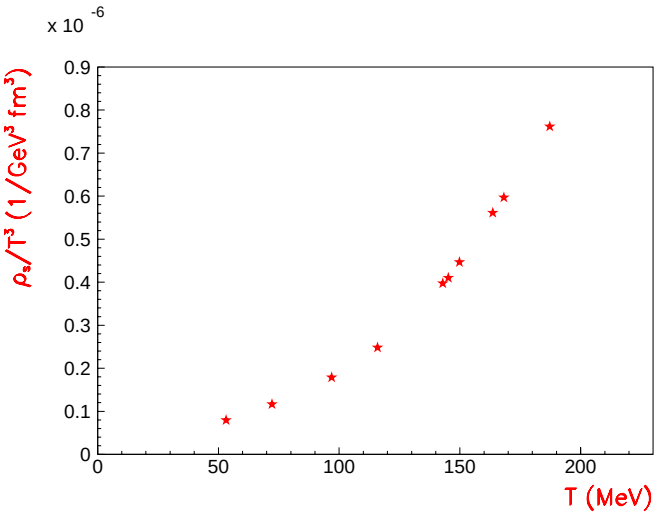

Fig. 18. The ratio of the entropy density to the temperature to the 3th power as a function of the temperature. The temperature is extrapolated to zero fugacities along an isentropic path for many nucleus+nucleus, hadron+hadron and lepton+lepton collisions. We demand for the thermal model fits a confidence level > 10%

Au collisions at 2 and 4 GeV per nucleon and of Pb + Pb collisions at 40 GeV per nucleon. We extrapolate these parameters to zero chemical potentials along an isentropic path and study the strangeness suppression factor λ_s ($\lambda_s = 2\overline{s}/(\overline{u}+\overline{d})$) as a function of the energy density reached early in each collision (initial energy density ϵ_i).

We arrive at the following conclusions:

(1) The so-called "strangeness suppression" puzzle, namely the decrease of the K^+/π^+ ratio measured in 4π acceptance (or equivalently of λ_s) with $s^{1/2}$ increasing from its value in Pb + Pb collisions at $40A$ GeV, is explained as reflecting the varying chemical potentials of the heavy ion systems.

(2) Several other experimental observations have the same origin:

(a) the increase of the double ratio $K/\pi(A+A/p+p)$ with decreasing $s^{1/2}$;

(b) the flatter behaviour of the K/π ratio as a function of $s^{1/2}$ when extracted at midrapidity;
the difference in the $s^{1/2}$ dependence of K^+/π^+ and K^-/π^- ratios;

(c) the enhancement seen in strange particles in central $p+A$ collisions as compared to $p+p$ collisions at the same $s^{1/2}$.

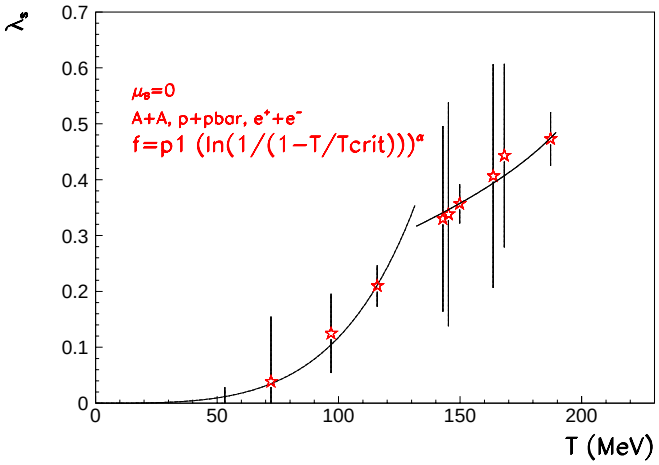

Fig. 19. The λ_s factor as a function of the temperature both extrapolated to zero fugacities along an isentropic path for many nucleus + nucleus, hadron + hadron and lepton + lepton collisions. We demand for the thermal model fits a confidence level > 10%. The lines shown are fits of the function $f = \beta[\ln(1/(1 - T/T_{\rm crit}))]^{\alpha}$ below and above $T = 140\,{\rm MeV}$. The fit of this function to the data above $T = 140\,{\rm MeV}$ gives $T_{\rm crit} = 218{\pm}70\,{\rm MeV}$, an exponent $\alpha = 0.54{\pm}0.47$ and $\chi^2/{\rm DOF} = 0.059/3$

(3) The λ_s value of systems with non-zero baryochemical potential is found to approach its limiting value at zero $\mu_{\rm B}$ as defined by the $p\overline{p}$ and e^+e^- colliding systems. We estimate that the limiting λ_s value (as well as an approximately net baryon free midrapidity region) will be reached by nuclear collisions at the initial energy density of $\sim$ 8–9 GeV/fm^3 (corresponding approximately to $s^{1/2} \sim$ 3–8 TeV per nucleon + nucleon pair) probably at the LHC.
(4) Strangeness is not significantly increased in nucleus–nucleus collisions as compared to elementary particle collisions, if they are compared (a) at the same (zero) chemical potential and (b) at the same initial energy density.
(5) However, λ_s is found to significantly increase in all systems which reach ϵ_i higher than $\sim 1\,{\rm GeV/fm^3}$, as compared to all systems below. Strangeness is found to follow closely the temperature, rising until $\epsilon_i \sim 1\,{\rm GeV/fm^3}$ and saturating along the border of the QCD phase transition, namely above $1\,{\rm GeV/fm^3}$. This allows us to extract in a model independent way the critical parameters of the QCD phase transition from the data, in particular, $\epsilon_{\rm critical} = 1 \pm 0.3\,{\rm GeV/fm^3}$ as well as the limiting T and λ_s values [4].
(6) Having established in Figs. 8 and 10 the critical initial energy density for the QCD phase transition of $\epsilon_{\rm crit} \sim 1 \pm 0.3\,{\rm GeV/fm^3}$, and determined the systems which go through the QGP phase, we study the way thermodynamic parameters approach the transition point.

We find that the systems with $\epsilon_i > 1\,{\rm GeV/fm^3}$, approach $T^{\rm fit}_{\rm crit} = 218 \pm 70\,{\rm MeV}$ with a (logarithmic) critical exponent $\alpha^{\rm fit} = 0.54 \pm 0.47$.

More data from SPS, RHIC and LHC at several values of $s^{1/2}$ will serve to narrow down the approach to the transition point.

Acknowledgements. I wish to thank the Schweizerische Nationalfonds for their support and P. Minkowski and K. Pretzl for discussions and critical comments.

References

1. A. Ali Khan et al., CP-PACS collaboration, hep-lat/0008011; F. Karsch, E. Laermann, A. Peikert, Ch. Schmidt, S. Stickan, hep-lat/0010027
2. J. Gasser, H. Leutwyler, Nucl. Phys. B **307**, 763 (1988)
3. P. Minkowski, Czech J. Phys. B **40**, 1003 (1990)
4. S. Kabana, P. Minkowski, hep-ph/0010247, to appear in New J. Phys.
5. Proceedings of Quark Matter conferences
6. R. Stock, Phys. Lett. B **456**, 277 (1999)
7. U. Heinz, M. Jacob, nucl-th/0002042
8. H. Satz, Rep. Prog. Phys. **63**, 1511 (2000)
9. D. Zschiesche et al., contribution to the Symposium on Fundamental Issues in Elementary Matter, 25–29 September 2000, Bad Honnef, Germany, nucl-th/0101047; S. Scherer et al., Prog. Part. Nucl. Phys. **42**, 279 (1999)
10. J. Rafelski, GSI Report 81-6, 282 (1981); J. Rafelski, R. Hagedorn, Statistical Mechanics of Quarks and Hadrons, edited by H. Satz (North Holland, Amsterdam 1981); J. Rafelski, Phys. Rep. **88**, 331 (1982); P. Koch, B. Mueller, J. Rafelski, Phys. Rep. **142**, 167 (1986)
11. S. Kabana, J. Phys. G **27**, 497 (2001), hep-ph/0010228; Proceedings of the XXX. International Conference on High Energy Physics, Osaka 2000, hep-ph/0010246
12. T. Matsui, H. Satz, Phys. Lett. B **178**, 416 (1986)
13. L. Gerland, L. Frakfurt, M. Strikman, H. Stocker, W. Greiner, J. Phys. G **27**, 695 (2001); M. Gorenstein, A.P. Kostyuk, H. Stocker, W. Greiner, hep-ph/0012015; P. Braun-Munzinger, J. Stachel, Phys. Lett. B **490**, 196 (2000); P. Csizmadia, P. Levai, hep-ph/0008195; P. Levai et al., hep-ph/0011023; R.L. Thews, M. Schroedter, J. Rafelski, hep-ph/0007323; J.P. Blaizot, M. Dinh, J.Y. Ollitrault, Phys. Rev. Lett. **85**, 4012 (2000); D. Kharzeev, R.L. Thews, Phys. Rev. C **60**, 041901 (1999), nucl-th/9907021; A. Capella, E. Ferreiro, A. Kaidalov, Phys. Rev. Lett. **85**, 2080 (2000)
14. M. Abreu et al. (NA50 coll.), Phys. Lett. B **477**, 28 (2000), CERN-EP-2000-013
15. S. Kabana, talk presented in the CERN Heavy Ion Forum, March 13th, 2001; hep-ph/0105152, to appear in the Proceedings of the XXXVIth Rencontres de Moriond on QCD and high energy hadronic interactions, 17–24 March 2001, Les Arcs 1800, France
16. P. Minkowski, W. Ochs, Eur. Phys. J. C **9**, 283 (1999), hep-ph/9811518; S. Kabana, P. Minkowski, Phys. Lett. B **472**, 155 (2000), hep-ph/9907570; Proceedings of the International Europhysics Conference on High Energy Physics (HEP'99), 15–21 July 1999, Tampere, Finland (IoP publishing), p. 862, hep-ph/9909351; P. Minkowski, S. Kabana, W. Ochs, Proceedings of the XXX International Conference on High Energy Physics (ICHEP'2000), 27 July–2 August 2000, Osaka, Japan, hep-ph/0011040
17. F. Becattini, J. Cleymans, A. Keränen, E. Suhonen, K. Redlich, hep-ph/0002267
18. R. Hagedorn, Nuovo Cim. Suppl. **3**, 147 (1965)
19. P. Gerber, H. Leutwyler, Nucl. Phys. B **321**, 387 (1989)

20. P. Braun-Munzinger, J. Stachel, Nucl. Phys. A **606**, 320 (1996), nucl-th/9606017
21. J. Letessier, J. Rafelski, nucl-th/0003014
22. T.S. Biro, P. Levai, J. Zimanyi, hep-ph/9807303
23. F. Becattini, A. Giovannini, S. Lupia, Z. Phys. C **72**, 491 (1996), hep-ph/9511203
24. F. Becattini, U. Heinz, Z. Phys. C **76**, 269 (1997), hep-ph/9702274
25. D. Rischke, to appear in the Proceedings of the QM2001, nucl-th/0104071
26. C. Pinkenburg et al. (E895 coll.), to appear in the Proceedings of the QM2001
27. L. Ahle et al. (E866 and E917 coll.), nucl-ex/0008010; B.B. Back et al. (E917 coll.), nucl-ex/0003007; L. Ahle et al. (E866 and E917 coll.), nucl-ex/9910008; R. Seto et al. (E917 coll.), Nucl. Phys. A **638**, 407 (1998)
28. N. Carrer et al. (NA57 coll.), to appear in the Proceedings of QM2001
29. F. Sikler (NA49 coll.), ISMD 2000, Tihany, Hungary, October 2000, hep-ex/0102004; C. Blume et al. (NA49 coll.), to appear in the Proceedings of QM2001
30. J.D. Bjorken, Phys. Rev. D **27**, 140 (1983)
31. S. Kabana, hep-ph/0004138, to appear in New J. Phys.
32. F. Antinori et al. (WA97 coll.), Phys. Lett. B **449**, 401 (1999); **433**, 209 (1998); C.A. Ogilvie et al. (E802 coll.), Nucl. Phys. A **630**, 571 (1998); L. Ahle et al. (E866 and E917 coll.), Phys. Lett. B **490**, 53 (2000); **476**, 1 (2000); R.A. Barton et al. (NA49 coll.), J. Phys. G **27**, 367 (2001); F. Sikler et al. (NA49 coll.), Nucl. Phys. A **661**, 45 (1999); S. Kabana et al. (NA52 coll.), J. Phys. G **27**, 495 (2001), hep-ex/0010053; paper submitted to ICHEP2000, hep-ex/0010045; G. Ambrosini et al. (NA52 coll.), New J. Phys. **1**, 22 (1999); **1**, 23 (1999); S. Kabana et al. (NA52 coll.), Nucl. Phys. A **661**, 370 (1999); J. Phys. G **25**, 217 (1999); G. Ambrosini et al. (NA52 coll.), Phys. Lett. B **417**, 202 (1998); S. Kabana et al. (NA52 coll.), J. Phys. G **23**, 2135 (1997); Nucl. Phys. A **638**, 411 (1998); R. Klingenberg et al. (NA52 coll.), Nucl. Phys. A **610**, 306 (1996); I. Bearden et al. (NA44 coll.), Phys. Lett. B **471**, 6 (1999) 12; D. Roehrich, J. Phys. G **27**, 355 (2001); W. Retyk et al. (NA35 coll.), J. Phys. G **23** 1845 (1997); T. Alber et al. (NA35 coll.), Z. Phys. C **64**, 195 (1994); Phys. Lett. B **366**, 56 (1996); J. Bächler et al. (NA35 coll.), Z. Phys. C **58**, 367 (1993); J. Bartke et al. (NA35 coll.), Z. Phys. C **48**, 191 (1990)
33. M. Gorenstein, M. Gazdzicki, Acta Phys. Pol. B **30**, 2705 (1999)
34. G. Torrieri, J. Rafelski, hep-ph/0103149; J. Rafelski et al., nucl-th/0101025; C. Greiner, nucl-th/0012093 and nucl-th/0009036; S. Soff et al., J. Phys. G **27**, 449 (2001), nucl-th/0010103; S. Hamieh et al., Phys. Lett. B **486**, 61 (2000), hep-ph/0006024; A. Capella, C.A. Salgado, hep-ph/0007236; M. Gazdzicki, D. Roehrich, Z. Phys. C **71** 55–64 (1996), hep-ex/9607004
35. K. Redlich, talk given in QM2001, to appear in the Proceedings, hep-ph/0105104
36. C.A. Ogilvie, to appear in the Proceedings of the QM2001
37. K. Pretzl et al. (NA52 coll.), contribution to the Symposium on Fundamental Issues in Elementary Matter, 25–29 September 2000, Bad Honnef, Germany, nucl-ex/0011016
38. S. Kabana, Ph.D. thesis, University of Frankfurt am Main, 1994
39. T. Susa et al. (NA49), to appear in the Proceedings of QM2001; B. Cole, to appear in the Proceedings of QM2001
40. Y. Ivanchenko, A. Lisyansky, Physics of critical fluctuations (Springer, 1995)
41. H. Stoecker, A.A. Ogloblin, W. Greiner, Z. Phys. A **303**, 259 (1981)